



# Temperature thresholds of ecosystem respiration at a global scale

Alice S. A. Johnston<sup>1,2</sup>✉, Andrew Meade<sup>2</sup>, Jonas Ardö<sup>3</sup>, Nicola Arriga<sup>4</sup>, Andy Black<sup>5</sup>, Peter D. Blanken<sup>6</sup>, Damien Bonal<sup>7</sup>, Christian Brümmer<sup>8</sup>, Alessandro Cescatti<sup>4</sup>, Jiří Dušek<sup>9</sup>, Alexander Graf<sup>10</sup>, Beniamino Gioli<sup>11</sup>, Ignacio Goded<sup>4</sup>, Christopher M. Gough<sup>12</sup>, Hiroki Ikawa<sup>13</sup>, Rachhpal Jassal<sup>5</sup>, Hideki Kobayashi<sup>14</sup>, Vincenzo Magliulo<sup>15</sup>, Giovanni Manca<sup>16</sup>, Leonardo Montagnani<sup>16,17</sup>, Fernando E. Moyano<sup>18</sup>, Jørgen E. Olesen<sup>19</sup>, Torsten Sachs<sup>20</sup>, Changliang Shao<sup>21</sup>, Torbern Tagesson<sup>3,22</sup>, Georg Wohlfahrt<sup>23</sup>, Sebastian Wolf<sup>24</sup>, William Woodgate<sup>25,26</sup>, Andrej Varlagin<sup>27</sup> and Chris Venditti<sup>2</sup>

**Ecosystem respiration is a major component of the global terrestrial carbon cycle and is strongly influenced by temperature. The global extent of the temperature–ecosystem respiration relationship, however, has not been fully explored. Here, we test linear and threshold models of ecosystem respiration across 210 globally distributed eddy covariance sites over an extensive temperature range. We find thresholds to the global temperature–ecosystem respiration relationship at high and low air temperatures and mid soil temperatures, which represent transitions in the temperature dependence and sensitivity of ecosystem respiration. Annual ecosystem respiration rates show a markedly reduced temperature dependence and sensitivity compared to half-hourly rates, and a single mid-temperature threshold for both air and soil temperature. Our study indicates a distinction in the influence of environmental factors, including temperature, on ecosystem respiration between latitudinal and climate gradients at short (half-hourly) and long (annual) timescales. Such climatological differences in the temperature sensitivity of ecosystem respiration have important consequences for the terrestrial net carbon sink under ongoing climate change.**

Carbon losses from terrestrial ecosystems determine the direction and magnitude of carbon–climate feedbacks<sup>1,2</sup>. The trajectory of future climate change therefore depends on the biological processes that underpin ecosystem fluxes. Ecosystem respiration ( $R_e$ ), the cumulative respiration of autotrophs (plants) and heterotrophs (bacteria, fungi and animals), represents a major component of the global carbon cycle<sup>3</sup>. Temperature strongly influences  $R_e$  through the laws of thermodynamics<sup>4–6</sup> but the global extent of the temperature– $R_e$  relationship has not been fully explored<sup>7,8</sup>.

Temperature-mediated variations in  $R_e$  are typically described as an exponential function in Earth system models (ESMs)<sup>2</sup>. That is, globally static  $Q_{10}$  values of around 2 represent a doubling of ecosystem  $CO_2$  fluxes with an increase in temperature of 10 °C, when all other terms are equal<sup>9</sup>. Empirical and theoretical studies,

however, have documented conflicting temperature– $R_e$  relationships. Latitudinal shifts in the temperature sensitivity of  $R_e$  have been observed in empirical studies, with ecosystems experiencing greater increases in  $R_e$  with temperatures at high, compared to low, latitudes<sup>8,10,11</sup>. At the same time, global syntheses have proposed convergent temperature sensitivities of  $R_e$  across different climates and ecosystem types<sup>4,12,13</sup>.

The influence of temperature on ecosystem respiration is mediated by the temperature sensitivity of individual physiology, community composition and biotic interactions of all the organisms inhabiting an ecosystem<sup>13,14</sup>. At the individual level, metabolic rates scale with body mass and increase exponentially with temperature according to the Boltzmann factor,  $e^{-E/kT}$ , where  $E$  is the activation energy (eV),  $k$  is the Boltzmann's constant ( $8.62 \times 10^{-5}$  eV K<sup>-1</sup>) and

<sup>1</sup>School of Water, Energy and Environment, Cranfield University, Bedford, UK. <sup>2</sup>School of Biological Sciences, University of Reading, Reading, UK. <sup>3</sup>Physical Geography and Ecosystem Science, Lund University, Lund, Sweden. <sup>4</sup>Joint Research Centre, European Commission, Ispra, Italy. <sup>5</sup>Faculty of Land and Food Systems, University of British Columbia, Vancouver, British Columbia, Canada. <sup>6</sup>Department of Geography, University of Colorado, Boulder, CO, USA. <sup>7</sup>Université de Lorraine, AgroParisTech, INRAE, UMR Silva, Nancy, France. <sup>8</sup>Thünen Institute of Climate-Smart Agriculture, Braunschweig, Germany. <sup>9</sup>Global Change Research Institute of the Czech Academy of Sciences, Brno, Czech Republic. <sup>10</sup>Institute for Bio- and Geosciences: Agrosphere (IBG-3), Forschungszentrum Jülich, Jülich, Germany. <sup>11</sup>Institute of Bioeconomy, CNR, Firenze, Italy. <sup>12</sup>Department of Biology, Virginia Commonwealth University, Richmond, VA, USA. <sup>13</sup>Institute for Agro-Environmental Sciences, National Agriculture and Food Research Organization, Tsukuba, Japan. <sup>14</sup>Research Institute for Global Change, Institute of Arctic Climate and Environment Research, Japan Agency for Marine-Earth Science and Technology, Tsukuba, Japan. <sup>15</sup>Institute for Mediterranean Agriculture and Forest Systems, CNR, Ercolano, Italy. <sup>16</sup>Autonomous Province of Bolzano, Forest Services, Bolzano, Italy. <sup>17</sup>Faculty of Science and Technology, Free University of Bolzano, Bolzano, Italy. <sup>18</sup>Bioclimatology, University of Goettingen, Göttingen, Germany. <sup>19</sup>Department of Agroecology, Aarhus University, Tjele, Denmark. <sup>20</sup>GFZ German Research Centre for Geoscience, Potsdam, Germany. <sup>21</sup>Institute of Agricultural Resources and Regional Planning, Chinese Academy of Agricultural Sciences, Beijing, China. <sup>22</sup>Department of Geosciences and Natural Resources, University of Copenhagen, Copenhagen, Denmark. <sup>23</sup>Department of Ecology, University of Innsbruck, Innsbruck, Austria. <sup>24</sup>Department of Environmental Systems Science, ETH Zurich, Zurich, Switzerland. <sup>25</sup>Land & Water, Commonwealth Scientific and Industrial Research Organisation, Canberra, Australian Capital Territory, Australia. <sup>26</sup>School of Earth and Environmental Sciences, The University of Queensland, Brisbane, Queensland, Australia. <sup>27</sup>A.N. Severtsov Institute of Ecology and Evolution, Russian Academy of Sciences, Moscow, Russia. ✉e-mail: [a.s.johnston@cranfield.ac.uk](mailto:a.s.johnston@cranfield.ac.uk)

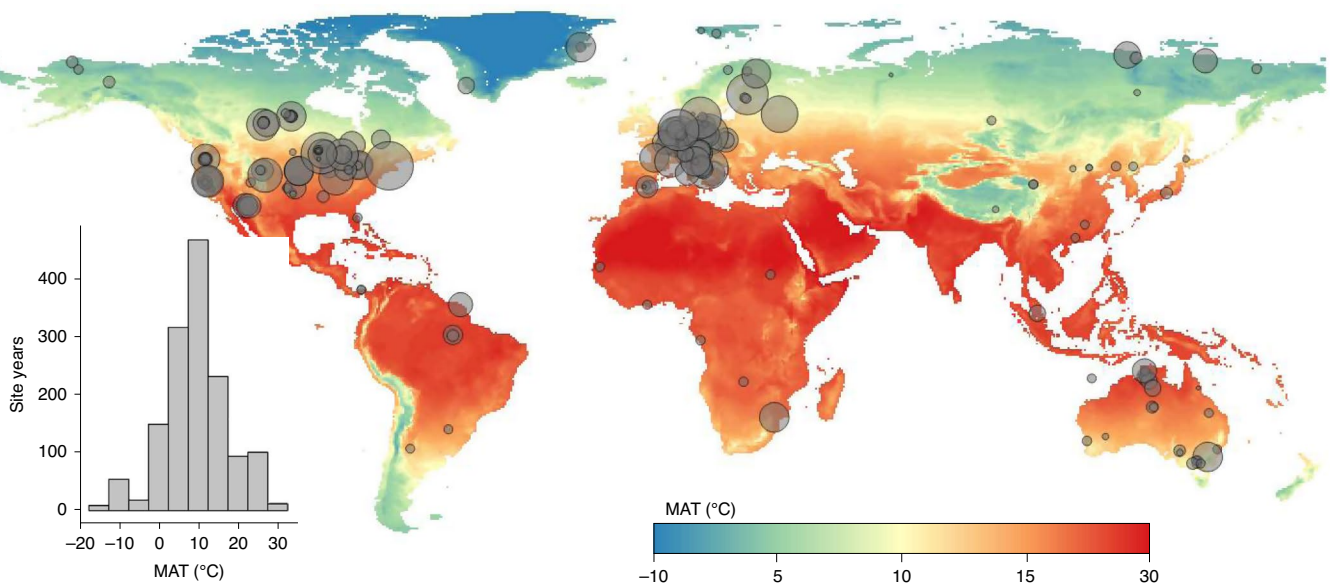


**Fig. 1 | Global distribution of the FLUXNET sites.** Site locations ( $n = 210$ ) are displayed over a world mean annual temperature (MAT) map<sup>40</sup>. Symbol diameter represents the number of site years (range 1–22 yr) and the inset left-hand figure shows the distribution of site years ( $n = 1,454$ ) by MAT. Map reproduced with permission from ref. <sup>40</sup>, The Nelson Institute Center for Sustainability and the Global Environment, University of Wisconsin-Madison; data source, Climate Research Unit, University of East Anglia.

$T$  is temperature (in Kelvin)<sup>6</sup>. Widescale application of the Boltzmann factor to individual metabolic rates has revealed a common value of  $E$  between 0.6 and 0.7 eV (refs. <sup>5,6,15</sup>). At the ecosystem level, models based on metabolic theory indicate exponential temperature– $R_e$  relationships across diverse ecosystems with a value of  $E$  surprisingly similar to individual metabolic rates (0.65 eV;  $Q_{10} \approx 2.50$ ; refs. <sup>4,13</sup>). Yet, models of the temperature– $R_e$  relationship have focused on a limited temperature range between 0 and 30°C, even though terrestrial ecosystems experience temperatures between –60 and 50°C (ref. <sup>16</sup>).

In this study we test the generality of the temperature– $R_e$  relationship, described by a general ecosystem model, across an extensive temperature range. The model, founded in metabolic theory, gives the linear expression:

$$\ln(R_e) = \frac{-E}{1,000k} \left( \frac{1,000}{T} \right) + \ln[(b_0)(C)] \quad (1)$$

where  $\ln(R_e)$  is the natural logarithm of ecosystem respiration, in  $\text{Wha}^{-1}$ ;  $(1,000/T)$  is the reciprocal of absolute temperature;  $b_0$  is the intensity of cellular metabolism; and  $C$  is the size distribution of organisms (assumed to be independent of  $R_e$  according to the energy equivalence rule<sup>4</sup>). The model predicts a general linear relationship between  $(1,000/T)$  and  $\ln(R_e)$ , with an expected slope ( $\bar{E}$  from hereon in) across diverse ecosystems equal to –7.50 K (0.65 eV, with a plausible range between –2 and –11 K or 0.2 and 1.2 eV)<sup>10</sup>. However, we would expect climatological differences in resource supply<sup>17,18</sup> and community composition<sup>14,19</sup> to alter  $\bar{E}$  across the global temperature range. We would also expect divergent relationships between metabolism and resource supply with temperature to modify the temperature– $R_e$  relationship over time<sup>13,20</sup>.

## Results

We test the global extent of the linear temperature– $R_e$  relationship predicted by metabolic theory, by applying the model presented in equation (1) to measurements across 210 globally distributed FLUXNET sites<sup>21</sup> (Fig. 1 and Supplementary Data 1). Both short-term (half-hourly) and long-term (annual) measurements

were tested for air and soil temperatures. The half-hourly FLUXNET dataset is presented with more conventional temperature and  $R_e$  units in Extended Data Fig. 1. The linear model (equation (1)) was compared to a threshold model, which accounts for variations in the activation energy ( $\bar{E}$ ) in equation (1) above and below specified temperature breakpoints (Methods). That is, the threshold model accounts for shifts in the temperature sensitivity of  $R_e$  across the global temperature range and explains latitudinal shifts in the temperature– $R_e$  relationship observed in empirical studies<sup>8,10,11</sup>. All models were linear mixed effects models and goodness of fit comparisons used Akaike Information Criterion (AIC) measurements.

The threshold model, which integrated two temperature breakpoints of  $-24.8 \pm 0.15$  and  $15.1 \pm 0.22$ °C, better explained  $R_e$  rates over the global extent of air temperatures in the FLUXNET dataset than the linear model ( $\Delta\text{AIC} = 3,839,265$ , Fig. 2). Similar to previous findings<sup>4,13</sup>, the threshold model indicates a temperature sensitivity of  $R_e$  indistinguishable from that of –7.50 K (0.65 eV, dashed line in Fig. 2a,b) predicted by metabolic theory (likelihood ratio test:  $\chi^2 = 0$ ,  $P = 1$ ) between temperature breakpoints ( $\bar{E} = -7.42$  K, 0.64 eV,  $Q_{10} \approx 2.45$  between 15.1 and –24.8°C, solid line in Fig. 2b). Evaluation of the linear model, on the other hand, gives an activation energy for global  $R_e$  rates of –7.30 K (0.63 eV, solid lines in Fig. 2a), significantly different from that predicted by metabolic theory (likelihood ratio test:  $\chi^2 = 20,009$ ,  $P < 0.0001$ ). Importantly, the threshold model indicates a lower temperature sensitivity of  $R_e$  at higher temperatures ( $\bar{E} = -2.84$  K, 0.25 eV,  $Q_{10} \approx 1.41 > 15.1$ °C) and extreme temperature sensitivity of  $R_e$  at very low temperatures ( $\bar{E} = -30.53$  K, 2.64 eV,  $Q_{10} \approx 40.79 < -24.8$ °C). The threshold model therefore primarily improves predictions, compared to the linear model, of the temperature– $R_e$  relationship at low and high latitude sites (Fig. 2f,g). High measured variability in  $R_e$  across the global temperature range, however, probably reflects the interactive effects of disturbance events, plant phenology and soil water and nutrient limitation on ecosystem metabolism.

Given the importance of belowground communities in  $R_e$  (refs. <sup>14,19</sup>), linear and threshold models were tested for the global relationship between soil temperature and ecosystem respiration (Fig. 2 and Supplementary Table 2). A single temperature threshold

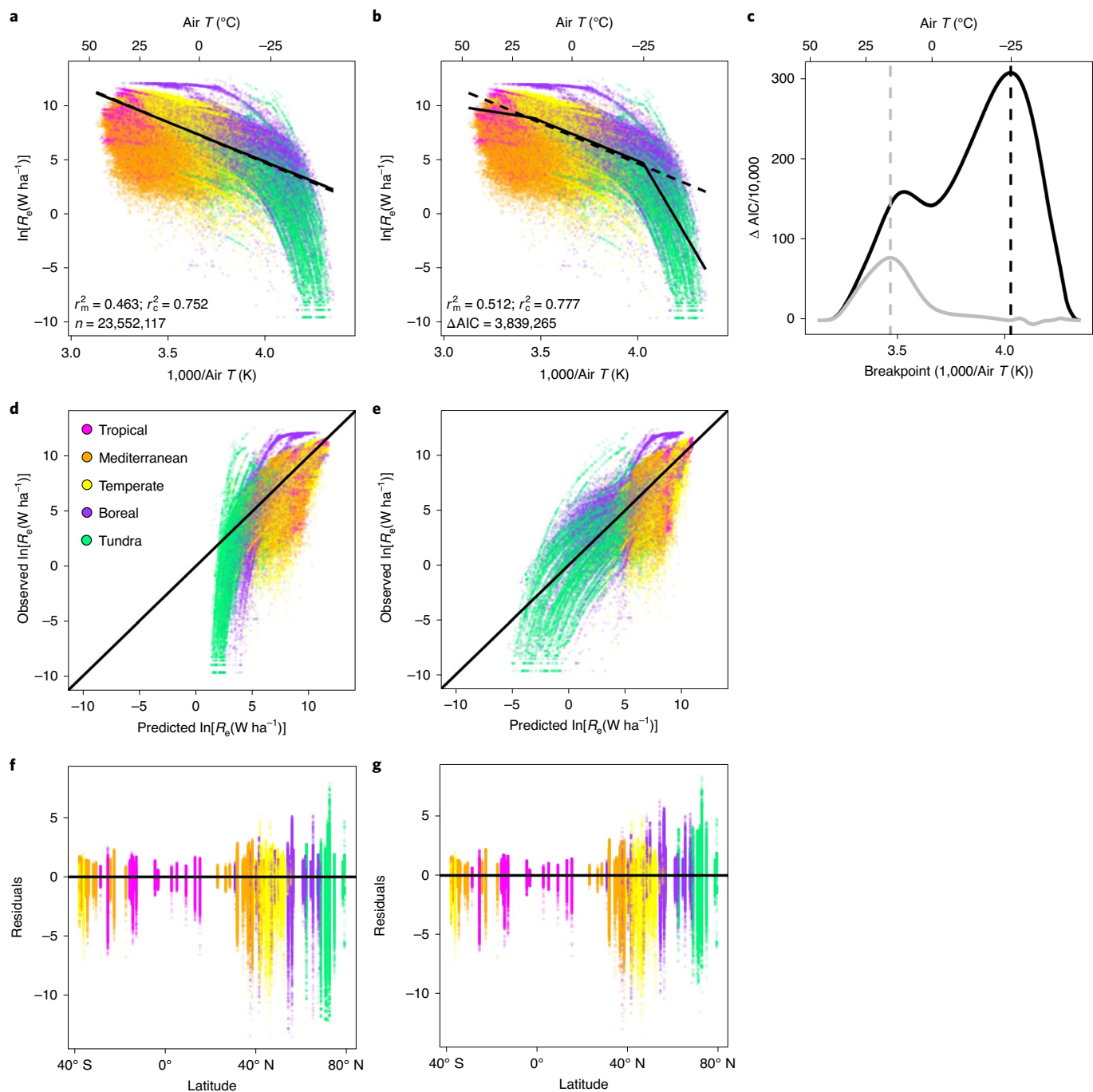


**Fig. 2 | Global extent of the temperature–ecosystem respiration ( $R_e$ ) relationship. a,b,d–g,** Night-time half-hourly ecosystem respiration measurements from the FLUXNET dataset (symbols), broadly classified as tropical (magenta), Mediterranean (orange), temperate (yellow), boreal (purple) or tundra (green) climates. Plots **a,d** and **f** present predictions from the linear model (equation (1)) and plots **b,e** and **g** present predictions from a threshold model with two temperature breakpoints (equation (2)), of the temperature–ecosystem respiration relationship. **c**, Plot shows the presence of two temperature breakpoints (black line: air (1,000/ $T$ ) = 4.027, –24.8 °C; grey line: air (1,000/ $T$ ) = 3.469, 15.1 °C), identified by the threshold models performance ( $\Delta AIC$ s compared to the linear model where higher values provide a better fit to the FLUXNET dataset). Goodness of fit measures indicate the pseudo  $r^2$  for marginal (fixed) effects ( $r_m^2$ ) and conditional (fixed and random) effects ( $r_c^2$ ), with **a** and **b** showing predictions of the fixed effects only (temperature, solid lines) in each model compared to the activation energy of –7.50 K predicted by metabolic theory (dashed lines,  $r_m^2 = 0.361$ ;  $r_c^2 = 0.542$ ). Plots **d** and **e** present model predictions against observed FLUXNET measurements (solid black 1:1 lines would demonstrate perfect prediction) and plots **f** and **g** show model residuals against latitude. Full details of the linear mixed effects models are presented in Supplementary Table 1.

of  $11.4 \pm 0.29$  °C emerged for soil temperature, with little evidence for a lower temperature breakpoint (likelihood ratio test:  $\chi^2 = 0$ ,  $P = 1$ ). Above the temperature threshold, the activation energy of  $R_e$  was lower than that observed for air temperature ( $\bar{E} = -2.18$  K,

$0.19$  eV,  $Q_{10} \approx 1.30$ ), while below the temperature threshold the activation energy was steeper than that between air temperature thresholds ( $\bar{E} = -13.37$  K,  $1.16$  eV,  $Q_{10} \approx 5.05$ ). The absence of a lower threshold for  $R_e$  with soil temperature is probably explained



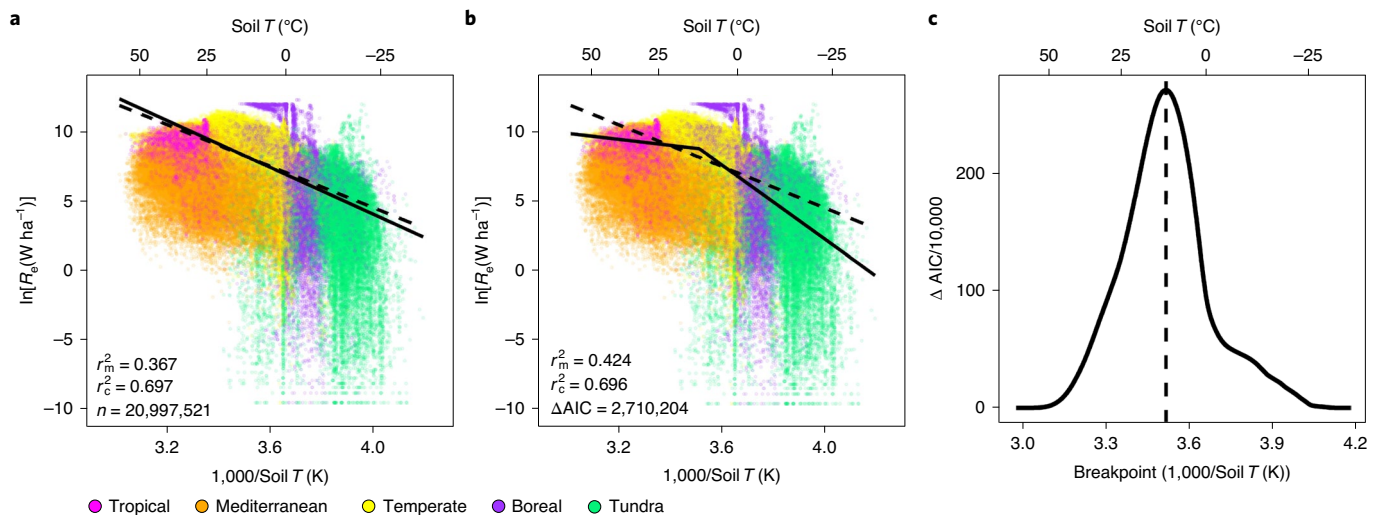


**Fig. 3 | The global soil temperature–ecosystem respiration relationship.** Night-time half-hourly ecosystem respiration measurements from the FLUXNET dataset (symbols), broadly classified by climate with symbol colours as in Fig. 2. **a, b**, Predictions of the temperature–ecosystem respiration relationship are compared for the linear model (**a**) and the threshold model (**b**), for the fixed effects of temperature (solid lines). Both models are compared to the activation energy of  $-7.50$  K predicted by metabolic theory (dashed lines,  $r_m^2 = 0.173$ ,  $r_c^2 = 0.500$ ). **c**, The plot shows the presence of a single temperature breakpoint (black line: soil  $(1,000/T) = 3.515$ ,  $11.4^\circ\text{C}$ ), identified by the threshold models performance ( $\Delta\text{AICs}$  compared to the linear model where higher values provide a better fit to the FLUXNET dataset). Full details of the linear mixed effects models are presented in Supplementary Table 2.

by thermal insulation from snow cover at low temperatures<sup>22</sup> resulting in much fewer observations, compared to air temperature, of the soil temperature– $R_e$  relationship below  $0^\circ\text{C}$ .

To account for the relative uncertainties of eddy covariance measurements below  $-20^\circ\text{C}$  (ref. <sup>23</sup>), alongside the emergence of a single temperature breakpoint for soil temperature, we tested the sensitivity of the air temperature threshold model to temperature ranges with few available measurements (Extended Data Fig. 2). Ecosystem respiration data were classified in  $5^\circ\text{C}$  temperature intervals and intervals containing  $<1\%$  of all measurements ( $n < 235,521$ ) were defined as low frequency intervals. Such intervals were present at both high ( $>36^\circ\text{C}$ ) and low ( $<-19^\circ\text{C}$ ) temperatures. Each low frequency temperature interval was removed one by one, as well as all together ( $\sim 1.8\%$  of the dataset), to investigate the sensitivity of the threshold model. The test provides supporting evidence of the robustness of temperature breakpoints to the removal of each temperature interval one by one. However, there was no support for a lower temperature breakpoint ( $-24.8^\circ\text{C}$  in Fig. 2b,c) when all low frequency intervals or all those  $<-19^\circ\text{C}$  were removed. Instead, a single temperature breakpoint of  $14.6^\circ\text{C}$  emerged (Extended Data Fig. 3 and Supplementary Table 3). The lower air temperature breakpoint should therefore be considered with caution until more accurate  $R_e$  measurements at low temperatures can be made.  $R_e$  rates nevertheless display a sharp decline at lower temperatures for both air (Fig. 2b) and soil (Fig. 3b) temperatures.

Sharp declines in  $R_e$  at low soil and air temperatures probably indicate pulse responses of soil respiration to rewetting and thawing events<sup>24</sup>, attributed to the suppression of microbial activity under water limitation in freezing conditions<sup>25</sup> and an uncoupling of the temperature dependence of microbial respiration from thermodynamic laws<sup>26</sup>. Differences between global temperature– $R_e$  relationships for air and soil temperature at short timescales also suggest shifts in the contribution of aboveground and belowground communities to  $R_e$  across the global extent of temperatures. For instance, a lower activation energy for the temperature– $R_e$  relationship at higher soil temperatures ( $\bar{E} = -2.18\text{ K} > 11.4 \pm 0.29^\circ\text{C}$ , Fig. 3), compared to air temperatures ( $\bar{E} = -2.84\text{ K} > 15.1^\circ\text{C}$ , Fig. 2), could indicate a relative reduction in the contribution of below-

ground autotrophs and heterotrophs to  $R_e$  in warmer climates. On the other hand, the lower threshold for the temperature– $R_e$  relationship at low air temperatures could reflect a temperature limit for the metabolism of aboveground communities, whereas the absence of a lower temperature threshold for soil temperature suggests the importance of belowground communities as components of  $R_e$  in mild to cold climates.

Global air temperature thresholds were consistent across climates but the goodness of fit of the threshold model (pseudo  $r^2$  and  $\Delta\text{AICs}$  compared to the linear model, Fig. 4) declined with a decrease in overall temperature range at lower latitudes. For instance, the temperature dependence of  $R_e$  (variation in  $R_e$  rates explained by temperature) was greater in cold, higher latitude and climates (tundra and boreal,  $r_m^2 > 0.60$ ), compared to mild (temperate,  $r_m^2 = 0.48$ ) and warm, low latitude and climates (Mediterranean and tropical,  $r_m^2 \leq 0.09$ ). In warmer climates, random effects had a much greater influence on  $R_e$  than in mild or cold climates, with FLUXNET site and latitude explaining more variation in tropical and Mediterranean ecosystems (Supplementary Table 4). Across the 210 sites, the threshold model better predicted the temperature– $R_e$  relationship in most cases ( $n = 197$ , Supplementary Data 1), while temperature explained more of the variation in  $R_e$  rates at sites with greater temperature ranges and higher latitudes (Extended Data Fig. 4).

$Q_{10}$  estimates from the threshold model reflect latitudinal shifts in the temperature sensitivity of ecosystem respiration, with tropical, Mediterranean, temperate, boreal and tundra climates yielding  $Q_{10}$  values of  $1.38 \pm 0.01$ ,  $1.82 \pm 0.43$ ,  $2.32 \pm 0.31$ ,  $2.67 \pm 0.10$  and  $2.90 \pm 0.12$ , respectively, compared to a global  $Q_{10}$  of  $2.26 \pm 0.35$  and higher  $Q_{10}$  estimates based on the soil temperature threshold model (Supplementary Table 5). Empirical observations of  $R_e$ , soil respiration and carbon turnover rates are comparable with threshold model estimates of higher temperature sensitivities of  $R_e$  at high latitudes and lower temperature sensitivities of  $R_e$  at low latitudes<sup>10,27</sup>. Weaker temperature control in the linear model, similar to ESMs that implement static global  $Q_{10}$  values, cannot capture shifts in  $R_e$  temperature sensitivities across the global temperature range (Supplementary Table 5).

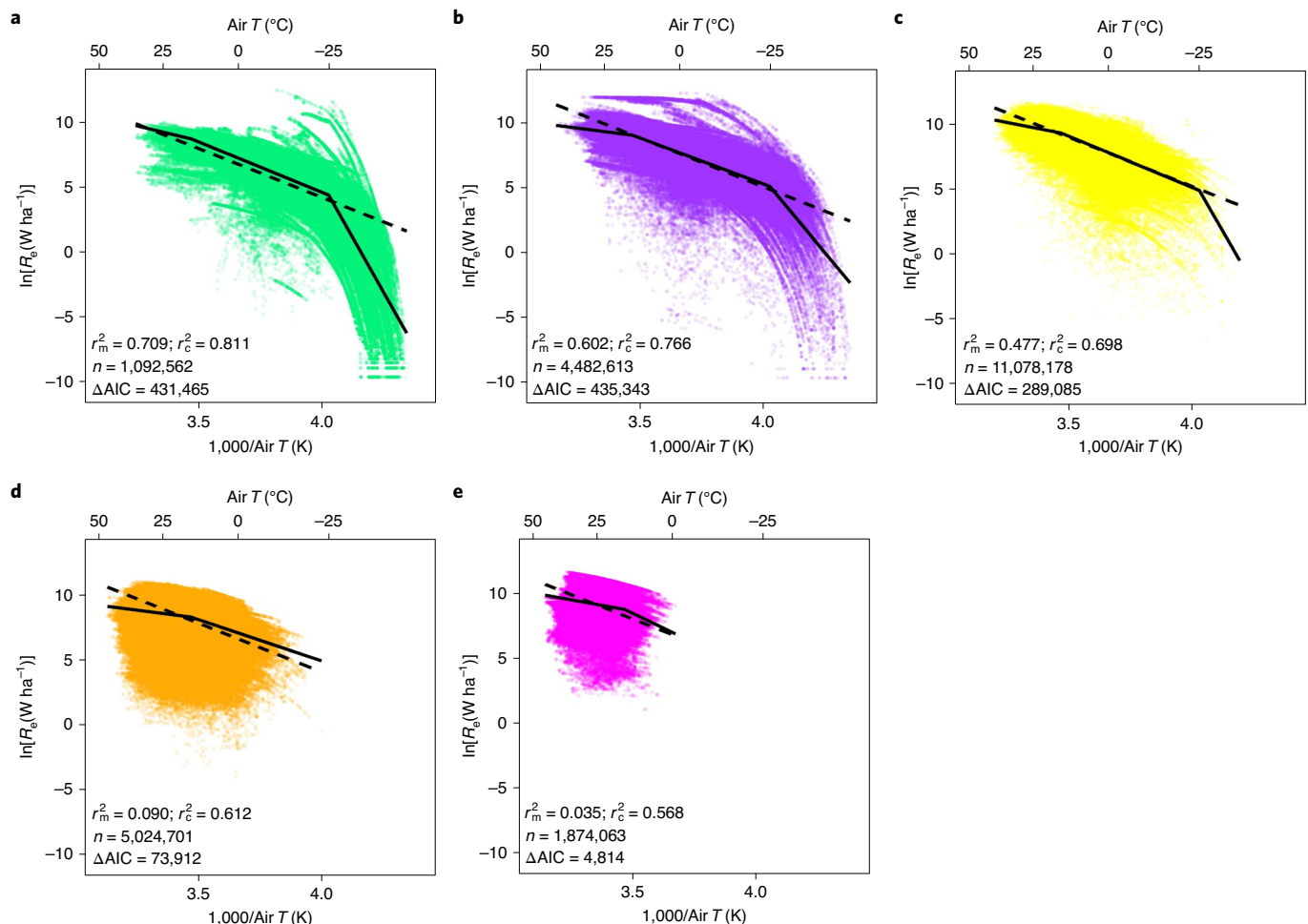


**Fig. 4 | Temperature thresholds of ecosystem respiration ( $R_e$ ) across five climates. a–e.** Night-time half-hourly ecosystem respiration measurements from the FLUXNET dataset (symbols), classified as **tundra (a)**, **boreal (b)**, **temperate (c)**, **Mediterranean (d)** and **tropical (e)**, with symbol colours as in Fig. 2. Solid lines show threshold model predictions for the fixed effects of temperature and dashed lines show an activation energy of  $-7.5$  K predicted by metabolic theory.  $\Delta AIC$ s indicate a greater goodness of fit of the threshold compared to linear model. Full details of the linear mixed effects models are presented in Supplementary Table 4.

Annual temperature– $R_e$  relationships were analysed across site years to investigate whether **climatological differences in the temperature dependence and sensitivity of  $R_e$  emerge over longer timescales**. The threshold model explained the temperature– $R_e$  relationship better than the linear model at longer timescales for both air and soil temperatures (Fig. 5). Surprisingly, threshold models converged for air and soil temperatures, with a single mid-temperature breakpoint of  $11.0 \pm 0.16^\circ\text{C}$  (Fig. 5b,d). Above the temperature threshold, annual  $R_e$  rates declined with increasing mean annual temperatures from mid to low latitudes, while the activation energy below the temperature threshold was markedly reduced (Fig. 5a,c,  $E \sim -4.90$  K,  $0.42$  eV) compared to short timescales. Weaker temperature relationships at longer timescales are reflected by global  $Q_{10}$  estimates of  $1.34 \pm 0.55$  and  $1.29 \pm 0.58$  for air and soil temperatures, respectively (Supplementary Table 6). An overall lack of  $R_e$  variation explained by temperature ( $r_m^2 < 0.14$ ) probably reflects the importance of confounding effects from soil water, nutrient limitation and resource availability, alongside thermal acclimation, at longer timescales. The threshold model was further consistent for annual soil respiration and air temperature measurements from the Global Soil Respiration Database<sup>28</sup>, with a single temperature breakpoint of  $5.5^\circ\text{C}$  (Extended Data Fig. 5 and Supplementary Table 6).

## Discussion

Our study shows how latitudinal shifts in  $R_e$  temperature sensitivity at both short and long timescales correspond to transitions in the global temperature– $R_e$  relationship across temperature thresholds. Importantly, temperature thresholds also indicate differences in the temperature dependence of  $R_e$ , with **more variation in  $R_e$  rates explained by temperature in cold compared to warm climates**. In cold climates, temperature strongly influences metabolic activity of belowground microbial communities<sup>19,25,26</sup>. In warm climates, ecosystem metabolism is limited by water and nutrient availability and resource availability to biological communities<sup>18,27,29–31</sup>.

Both the temperature sensitivity and dependence of annual  $R_e$  rates are markedly reduced compared to the short-term  $R_e$  temperature response, suggesting the dominance of resource effects on ecosystem metabolism at longer timescales<sup>13</sup>. For instance, primary production directs carbon availability for ecosystem metabolism and typically shows a weaker temperature dependence<sup>20,32</sup>. Nutrient availability further drives preferential allocation of photosynthate C aboveground or belowground, with consequences for carbon availability and quality to different ecosystem components<sup>17</sup>.

Thresholds to the temperature– $R_e$  relationship shown here will undoubtedly result from temporally divergent sensitivities between ecosystem components (for example, belowground and

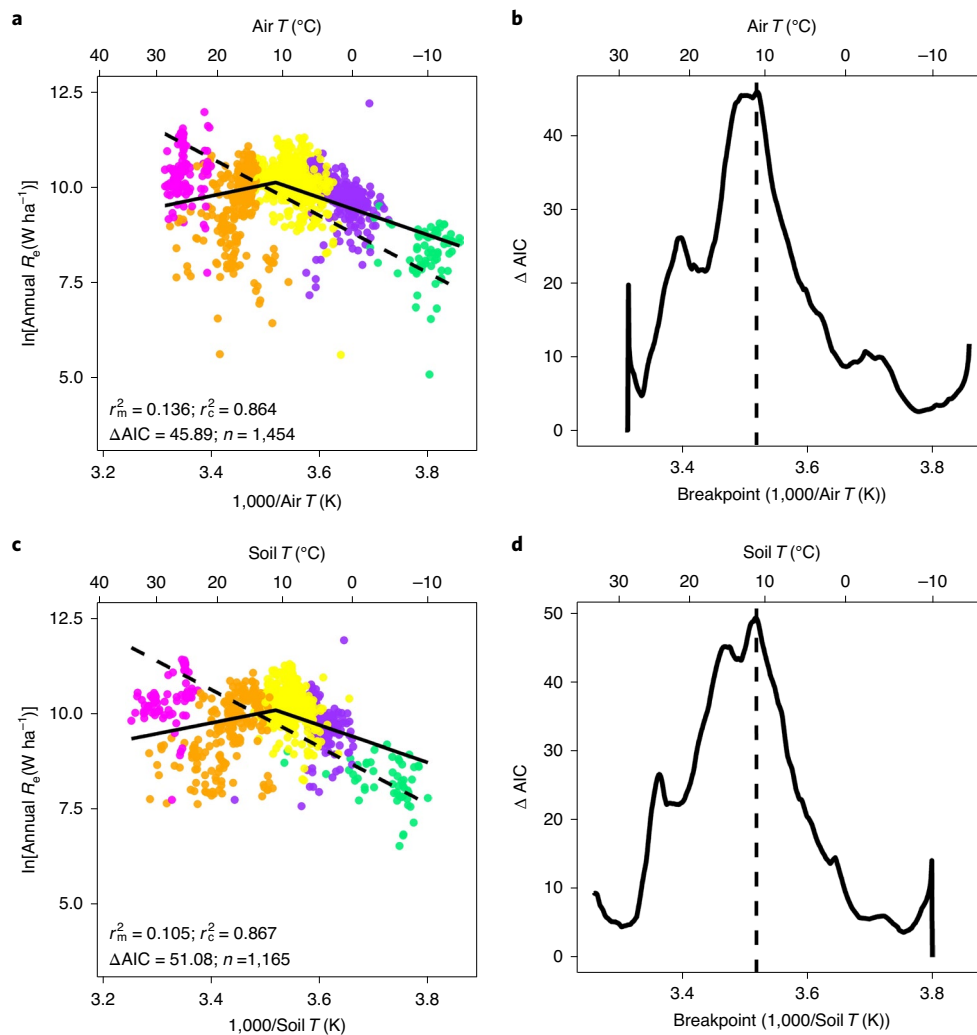


**Fig. 5 | Long-term temperature thresholds of ecosystem respiration ( $R_e$ ).** **a,c**, Mean annual  $R_e$  and either air (**a**) or soil (**c**) temperature measurements (symbols), with symbol colours representing climate as in Fig. 2. Plots show predictions from the threshold model (solid lines, for the fixed effects of temperature only), with dashed lines indicating an activation energy of  $-7.50 \text{ K}$  as predicted by metabolic theory. **b,d**, Both threshold models identified a single temperature breakpoint of  $11.0^\circ\text{C}$  (dashed lines), with little support for a second temperature breakpoint ( $\Delta\text{AIC} < 5$  and  $P > 0.05$ ).  $\Delta\text{AIC}$ s are between the linear and threshold models. Full details of the threshold mixed effects models are presented in Supplementary Table 6.

aboveground, heterotrophic and autotrophic) and several environmental controls over time. Variable acclimation of the different components of  $R_e$  to these environmental controls may further influence the temperature dependence and sensitivity of  $R_e$  by modifying the temperature response of catabolic and anabolic pathways<sup>33–35</sup>. Although we would expect such mechanisms to occur as gradual state changes rather than the sharp breakpoints described here, our study indicates consistent temperature thresholds at which ecosystem metabolism changes at a global scale. However, such results need to be validated for different ecosystem components as detailed measurements become available and for decadal timescales over which the influence of anthropogenic factors can be detected.

Biosphere feedbacks with future climate changes will be strongly influenced by the temperature– $R_e$  relationship<sup>36,37</sup> and latitudinal shifts in  $R_e$  temperature sensitivity as identified here will have important consequences for the global net land carbon sink<sup>38</sup>. For instance, while huge stores of labile carbon in permafrost regions could be released if temperatures rise above lower thresholds for microbial decomposition<sup>26</sup>,  $\text{CO}_2$  fertilisation in tropical and boreal regions could enhance carbon gains through primary production relative to losses through  $R_e$  (refs. <sup>30,39</sup>). Climate change forecasts

by ESMs would thus be improved by accounting for temperature thresholds of  $R_e$  at a global scale. A higher resolution understanding of  $R_e$ –climate feedbacks, however, requires strategic disentangling of the multiple environmental controls on the aboveground, belowground, heterotrophic and autotrophic components of terrestrial ecosystem carbon fluxes.

## Methods

**The FLUXNET dataset.** FLUXNET is a global network of micrometeorological sites providing eddy covariance  $\text{CO}_2$  exchange observations between terrestrial ecosystems and the atmosphere<sup>21</sup>. The FLUXNET 2015 dataset used in this study provides half-hourly temperature and night-time  $R_e$  measurements over 1,454 site years and a latitudinal range of  $78.92^\circ\text{N}$  to  $37.43^\circ\text{S}$ . Observations across the 210 sites, which range from arctic tundra to tropical rainforest ecosystems, provide an extensive temperature range of  $89.7^\circ\text{C}$ , from  $-43.4$  to  $46.3^\circ\text{C}$  (Fig. 1 and Supplementary Data 1).

The FLUXNET dataset is subject to a data processing pipeline which include data quality controls checks, filtering of low turbulence periods and partitioning of  $\text{CO}_2$  fluxes into respiration and photosynthesis components using established methods<sup>21</sup>. Disentangling respiration and photosynthesis fluxes during the day is complex and the extraction of  $R_e$  relies on modelling techniques with high uncertainty. Night-time  $\text{CO}_2$  exchange measurements thus provide the best approximation of  $R_e$  and uncertainty has been minimised for the FLUXNET

dataset by using quality control procedures<sup>21</sup>. Here, non-gap-filled half-hourly ( $\mu\text{mol CO}_2 \text{ m}^{-2} \text{ s}^{-1}$ ) and annual ( $\text{g C m}^{-2}$ ) night-time  $R_e$  (RECO\_NT\_VUT\_MEAN), air temperature (TA\_F) and soil temperature (TS\_F) measurements were compiled from the FLUXNET 2015 dataset (<https://fluxnet.fluxdata.org/data/fluxnet2015-dataset/>).  $R_e$  measurements were then converted to units of metabolic energy ( $\text{W ha}^{-1}$ ) (ref. <sup>4</sup>) by taking  $0.272 \text{ J } \mu\text{mol CO}_2$  and  $10,000 \text{ m}^2 \text{ ha}^{-1}$ .

**Model analysis.** The linear model (equation (1)) for describing the temperature– $R_e$  relationship was fitted to the global FLUXNET dataset, for both air and soil temperature. To test for the presence of temperature thresholds to the linear temperature– $R_e$  model at a global scale, which explain shifts in  $R_e$  temperature sensitivity across climates, we compare the linear model in equation (1) to a threshold (piecewise) model. The threshold model, with two temperature breakpoints, gives:

$$\ln(R_e) = \bar{E}_1 f_1(1,000/T, k_1) + \bar{E}_2 f_2(1,000/T, k_1, k_2) + \bar{E}_3 f_3(1,000/T, k_2) + \ln[(b_0)(C)] \quad (2)$$

where  $\bar{E}_1$ ,  $\bar{E}_2$  and  $\bar{E}_3$  represent activation energies for different temperature ( $1,000/T$ ) ranges, determined by the two temperature breakpoints ( $k_1$  and  $k_2$ ) and  $f$  represents the functions:

$$f_1 = \begin{cases} 1,000/T, & 1,000/T \leq k_1 \\ k_1, & k_1 > 1,000/T \end{cases}$$

$$f_2 = \begin{cases} 0, & 1,000/T \leq k_1 \\ 1,000/T - k_1, & k_1 \leq 1,000/T \leq k_2 \\ k_2 - k_1, & 1,000/T > k_2 \end{cases}$$

$$f_3 = \begin{cases} 0, & 1,000/T \leq k_2 \\ 1,000/T, & 1,000/T > k_2 \end{cases}$$

The threshold model first introduced a single temperature breakpoint to the linear model, so that the activation energy ( $\bar{E}$ , with more negative values indicating higher temperature sensitivity) varies above and below a specified temperature. Temperature breakpoints were tested for the temperature ( $1,000/T$ ) range between 3.1 and 4.4, for every increment of 0.001 ( $\sim 0.07^\circ\text{C}$ ). Differences in linear and threshold model AICs were then compared for every temperature breakpoint. The highest  $\Delta\text{AIC}$  was taken as providing the most support for a temperature breakpoint, as long as  $\Delta\text{AIC} > 5$  for additional degrees of freedom and  $P < 0.05$  in a likelihood ratio test. Then, the threshold model integrated an additional temperature breakpoint, taking the first temperature breakpoint with the greatest support as a fixed value. Model AICs for each second temperature breakpoint were compared to the single threshold model and the second threshold was selected on the basis of the highest  $\Delta\text{AIC}$  given the conditions outlined above. Temperature breakpoints were identified for short (half-hourly) and long (annual) temperature– $R_e$  relationships.

All models were linear mixed effects models, with FLUXNET site and latitude set as random effects. First, the models were tested for the global dataset and then for broadly classified climate zones (cold, mild and warm) and climates (tundra, boreal, temperate, Mediterranean and tropical). Some generalisations were necessary during climate classification. For instance, alpine sites at mid-latitudes were classified as boreal climates (Supplementary Data 1). Linear and threshold models were further tested for each FLUXNET site. Finally, annual  $R_e$  rates were used to investigate changes in temperature breakpoints and linear and threshold model performance, at long timescales for air and soil temperature. Long timescale models accounted for latitude and year as random effects.

**Reporting Summary.** Further information on research design is available in the Nature Research Reporting Summary linked to this article.

## Data availability

The data analysed during the current study are available on the FLUXNET website (<https://fluxnet.fluxdata.org/data/fluxnet2015-dataset/>) and are subject to data policy restrictions (<https://fluxnet.org/data/data-policy>). Summaries for each FLUXNET site are provided in Supplementary Data 1.

## Code availability

The R code used for analysis during the current study is available on Zenodo (<https://doi.org/10.5281/zenodo.4506798>).

Received: 21 August 2020; Accepted: 14 January 2021;

Published online: 22 February 2021

## References

1. Cao, M. & Woodward, F. I. Dynamic responses of terrestrial ecosystem carbon cycling to global climate change. *Nature* **393**, 249–252 (1998).

2. Heimann, M. & Reichstein, M. Terrestrial ecosystem carbon dynamics and climate feedbacks. *Nature* **451**, 289–292 (2008).
3. Allen, A. P., Gillooly, J. F. & Brown, J. H. Linking the global carbon cycle to individual metabolism. *Funct. Ecol.* **19**, 202–213 (2005).
4. Enquist, B. J. et al. Scaling metabolism from organisms to ecosystems. *Nature* **423**, 639–642 (2003).
5. Gillooly, J. F., Brown, J. H., West, G. B., Savage, V. M. & Charnov, E. L. Effects of size and temperature on metabolic rate. *Science* **293**, 2248–2251 (2001).
6. Brown, J. H., Gillooly, J. F., Allen, A. P., Savage, V. M. & West, G. B. Toward a metabolic theory of ecology. *Ecology* **85**, 1771–1789 (2004).
7. Friedlingstein, P. et al. Uncertainties in CMIP5 climate projections due to carbon cycle feedbacks. *J. Clim.* **27**, 511–526 (2014).
8. Davidson, E. A. & Janssens, I. A. Temperature sensitivity of soil carbon decomposition and feedbacks to climate change. *Nature* **440**, 165–173 (2006).
9. Lenton, T. M. & Huntingford, C. Global terrestrial carbon storage and uncertainties in its temperature sensitivity examined with a simple model. *Glob. Change Biol.* **9**, 1333–1352 (2003).
10. Song, B. et al. Divergent apparent temperature sensitivity of terrestrial ecosystem respiration. *J. Plant Ecol.* **7**, 419–428 (2014).
11. Lloyd, J. & Taylor, J. A. On the temperature dependence of soil respiration. *Funct. Ecol.* **8**, 315–323 (1994).
12. Mahecha, M. D. et al. Global convergence in the temperature sensitivity of respiration at ecosystem level. *Science* **329**, 838–840 (2010).
13. Yvon-Durocher, G. et al. Reconciling the temperature dependence of respiration across timescales and ecosystem types. *Nature* **487**, 472–476 (2012).
14. Johnston, A. S. A. & Sibly, R. M. The influence of soil communities on the temperature sensitivity of soil respiration. *Nat. Ecol. Evol.* **2**, 1597–1602 (2018).
15. Dell, A. I., Pawar, S. & Savage, V. M. Systematic variation in the temperature dependence of physiological and ecological traits. *Proc. Natl Acad. Sci. USA* **108**, 10591–10596 (2011).
16. Buckley, L. B. & Huey, R. B. Temperature extremes: geographic patterns, recent changes, and implications for organismal vulnerabilities. *Glob. Change Biol.* **22**, 3829–3842 (2016).
17. Gill, A. L. & Finzi, A. C. Belowground carbon flux links biogeochemical cycles and resource-use efficiency at the global scale. *Ecol. Lett.* **19**, 1419–1428 (2016).
18. Green, J. K. et al. Large influence of soil moisture on long-term terrestrial carbon uptake. *Nature* **565**, 476–479 (2019).
19. Allison, S. D., Wallenstein, M. D. & Bradford, M. A. Soil-carbon response to warming dependent on microbial physiology. *Nat. Geosci.* **3**, 336–340 (2010).
20. Michaletz, S. T., Cheng, D., Kerkhoff, A. J. & Enquist, B. J. Convergence of terrestrial plant production across global climate gradients. *Nature* **512**, 39–43 (2014).
21. Pastorello, G. et al. The FLUXNET2015 dataset and the ONEFlux processing pipeline for eddy covariance data. *Sci. Data* **7**, 225 (2020).
22. Monson, R. K. et al. Winter forest soil respiration controlled by climate and microbial community composition. *Nature* **439**, 711–714 (2006).
23. Mauder, M. et al. A strategy for quality and uncertainty assessment of long-term eddy-covariance measurements. *Agric. Meteorol.* **169**, 122–135 (2013).
24. Kim, D.-G., Vargas, R., Bond-Lamberty, B. & Turetsky, M. R. Effects of soil rewetting and thawing on soil gas fluxes: a review of current literature and suggestions for future research. *Biogeosciences* **9**, 2459–2483 (2012).
25. Du, E. et al. Winter soil respiration during soil-freezing process in a boreal forest in Northeast China. *J. Plant Ecol.* **6**, 349–357 (2013).
26. Schuur, E. A. et al. Climate change and the permafrost carbon feedback. *Science* **520**, 171–179 (2015).
27. Koven, C. D., Hugelius, G., Lawrence, D. M. & Wieder, W. R. Higher climatological temperature sensitivity of soil carbon in cold than warm climates. *Nat. Clim. Change* **7**, 817–822 (2017).
28. Bond-Lamberty, B. P. & Thomson, A. M. A Global Database of Soil Respiration Data Version 4.0 (ORNL DAAC, 2018); <https://doi.org/10.3334/ORNLDAAC/1578>
29. Zhang, Z. et al. A temperature threshold to identify the driving climate forces of the respiratory process in terrestrial ecosystems. *Eur. J. Soil Biol.* **89**, 1–8 (2018).
30. Yang, Y., Donohue, R. J., McVicar, T. R., Roderick, M. L. & Beck, H. E. Long-term CO<sub>2</sub> fertilization increases vegetation productivity and has little effect on hydrological partitioning in tropical rainforests. *J. Geophys. Res. Biogeosci.* **121**, 2125–2140 (2016).
31. Fleischer, K. et al. Amazon forest response to CO<sub>2</sub> fertilization dependent on plant phosphorus acquisition. *Nat. Geosci.* **12**, 736–741 (2019).
32. Padfield, D. et al. Metabolic compensation constrains the temperature dependence of gross primary production. *Ecol. Lett.* **20**, 1250–1260 (2017).
33. Atkin, O. K. & Tjoelker, M. G. Thermal acclimation and the dynamic response of plant respiration to temperature. *Trends Plant Sci.* **8**, 343–351 (2003).



34. Huntingford, C. et al. Implications of improved representations of plant respiration in a changing climate. *Nat. Commun.* **8**, 1602 (2017).
35. Niu, S. et al. Thermal optimality of net ecosystem exchange of carbon dioxide and underlying mechanisms. *New Phytol.* **194**, 775–783 (2012).
36. Rind, D. The consequences of not knowing low- and high-latitude climate sensitivity. *Bull. Am. Meteorol. Soc.* **89**, 855–864 (2008).
37. Liu, Z. et al. Increased high-latitude photosynthetic carbon gain offset by respiration carbon loss during an anomalous warm winter to spring transition. *Glob. Change Biol.* **26**, 682–696 (2020).
38. Haverd, V. et al. Higher than expected CO<sub>2</sub> fertilization inferred from leaf to global observations. *Glob. Change Biol.* **26**, 2390–2402 (2020).
39. Tagesson, T. et al. Recent divergence in the contributions of tropical and boreal forests to the terrestrial carbon sink. *Nat. Ecol. Evol.* **4**, 202–209 (2020).
40. Climate Research Unit, University of East Anglia *Average Annual Temperature. Atlas Biosphere* (Center for Sustainability and the Global Environment, accessed 6 February 2020); <https://nelson.wisc.edu/sage/data-and-models/atlas/maps.php>

## Acknowledgements

This work used eddy covariance data acquired and shared by the FLUXNET community and was supported by a Leverhulme Trust Research Project Grant (RPG-2017-071) and a Leverhulme Trust Research Leadership Award (RL-2019-012) to C.V. A.M. was supported by BBSRC (BB/S019952/1) and the Leverhulme Trust (RPG-2019-170), P.D.B. by the US Department of Energy Office of Science (7094866), D.B. by French Agence Nationale de la Recherche (ANR-10-LABX-25-01; ANR-11-LABX-0002-01), J.D. by the Ministry of Education, Youth and Sports of the Czech Republic (LM2015061), C.G. by a National Science Foundation Award (1655095) and A.V. by Russian Foundation for

Basic Research project 19-04-01234-a. We also thank J. Baker, G. Butler and A. Navarro Campoy for helpful discussions.

## Author contributions

A.S.A.J. and C.V. developed the methodology and led the writing of the manuscript. A.S.A.J. and A.M. conducted the data analysis. J.A., N.A., D.B., A.B., P.D.B., C.B., A.C., J.D., A.G., B.G., I.G., C.M.G., H.I., R.J., H.K., V.M., G.M., L.M., F.E.M., J.E.O., T.S., C.S., T.T., G.W., S.W., W.W. and A.V. contributed data. All authors contributed to manuscript revisions.

## Competing interests

The authors declare no competing interests.

## Additional information

**Extended data** is available for this paper at <https://doi.org/10.1038/s41559-021-01398-z>.

**Supplementary information** The online version contains supplementary material available at <https://doi.org/10.1038/s41559-021-01398-z>.

**Correspondence and requests for materials** should be addressed to A.S.A.J.

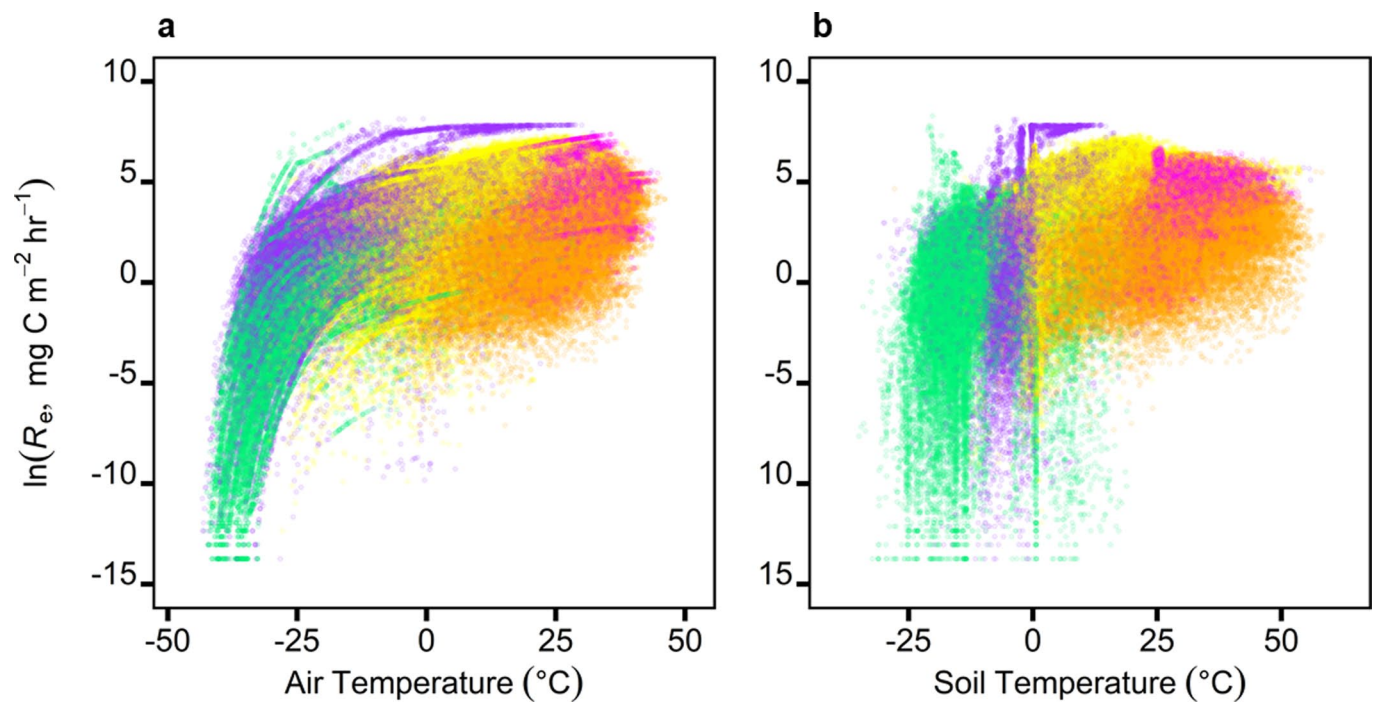
**Peer review information** *Nature Ecology & Evolution* thanks Chris Huntingford and the other, anonymous, reviewer(s) for their contribution to the peer review of this work. Peer reviewer reports are available.

**Reprints and permissions information** is available at [www.nature.com/reprints](http://www.nature.com/reprints).

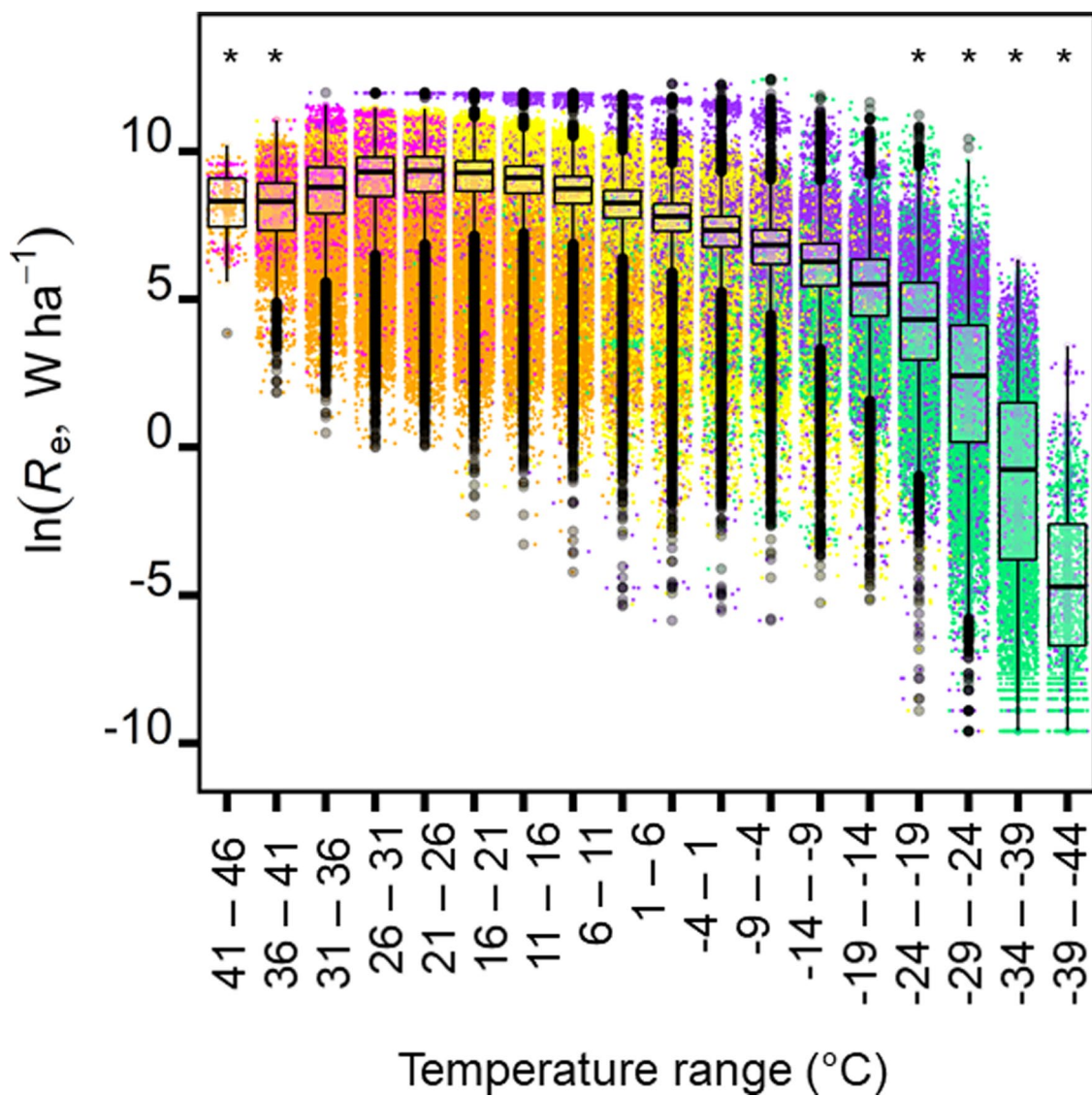
**Publisher's note** Springer Nature remains neutral with regard to jurisdictional claims in published maps and institutional affiliations.

© The Author(s), under exclusive licence to Springer Nature Limited 2021

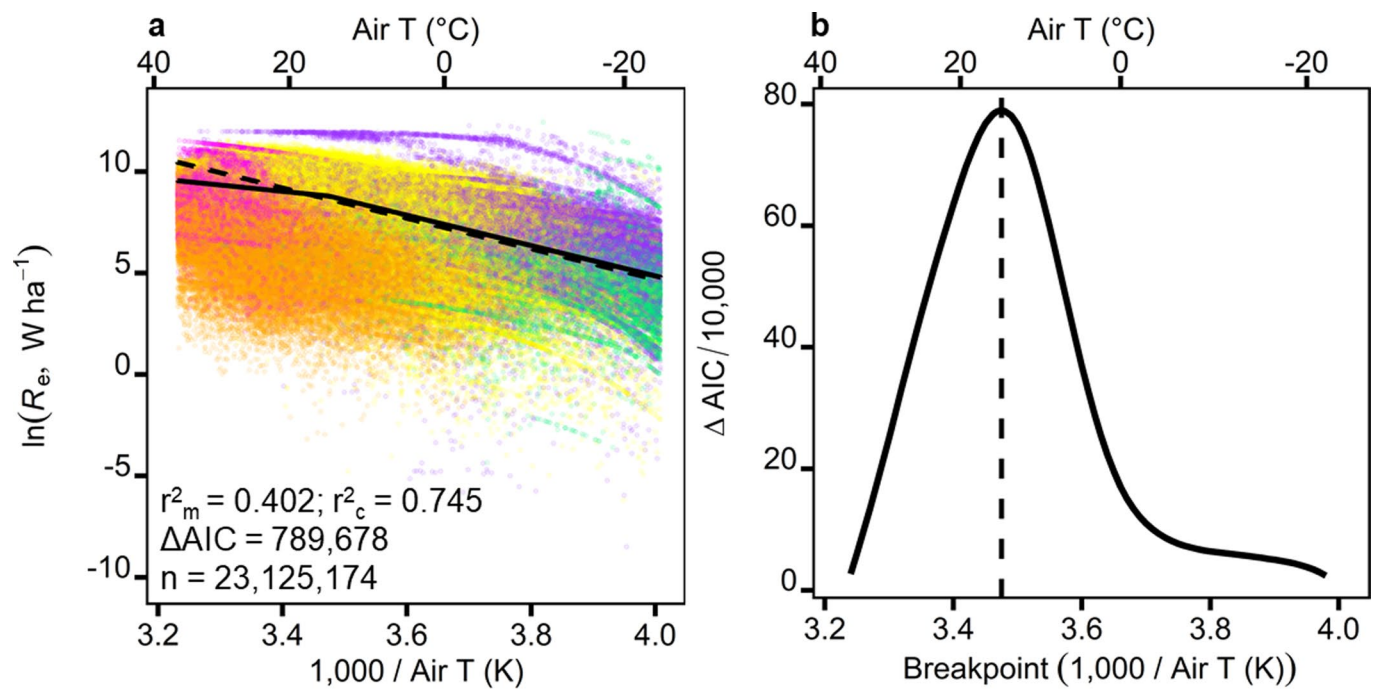




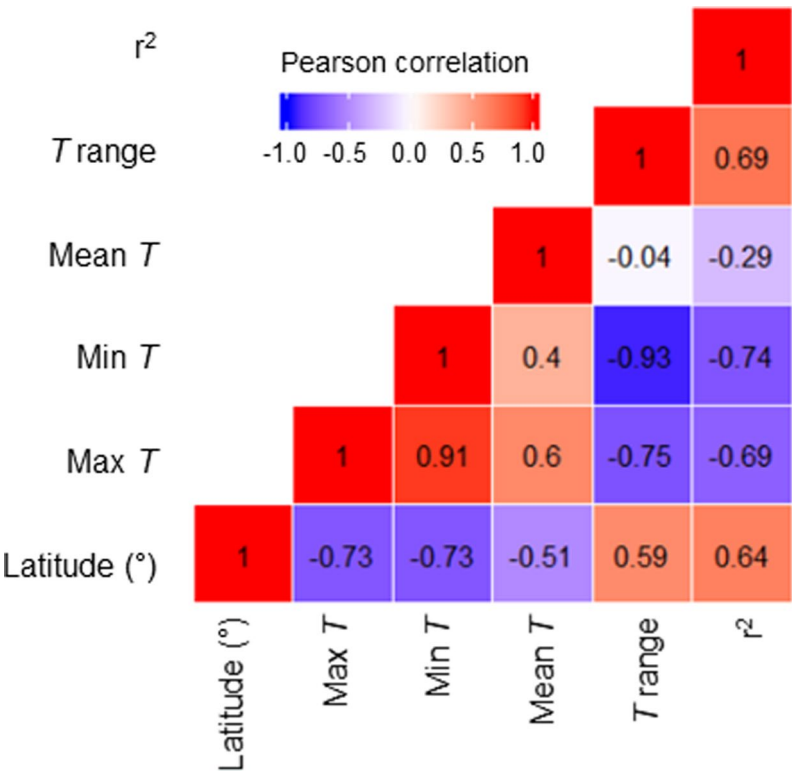
**Extended Data Fig. 1 | Short-term temperature and ecosystem respiration measurements in conventional units.** Night-time half-hourly ecosystem respiration measurements from the FLUXNET dataset (symbols, colours representing climate as in Fig. 2) for a) air and b) soil temperature. Plots show ecosystem respiration rates in  $\text{mg C m}^{-2} \text{ hr}^{-1}$  and temperature in degrees Celsius units.



**Extended Data Fig. 2 | Identification of low frequency air temperature intervals.** Boxplot of the half-hourly ecosystem respiration measurements from the FLUXNET dataset (symbols, colours representing climate as in Fig. 2) presented in 5°C air temperature intervals. Boxplots show median values (centre lines) and upper and lower quantiles, with black symbols representing outliers. Asterisks at the top indicate extreme high and low 5°C temperature intervals with few measurements (< 1 % of the dataset,  $n < 235,521$ ). The temperature intervals with asterisks (low frequency intervals) were removed from the dataset one by one as well as all together and the threshold model tested. The temperature breakpoints were robust to the removal of each temperature interval one by one but there was no support for a cold temperature breakpoint ( $-24.8^{\circ}\text{C}$  in Fig. 2b,c) when all low frequency intervals or all those  $< -19^{\circ}\text{C}$  were removed. A single temperature breakpoint emerged from the threshold model when all low frequency intervals were removed (Extended Data Fig. 3 and Supplementary Table 3).

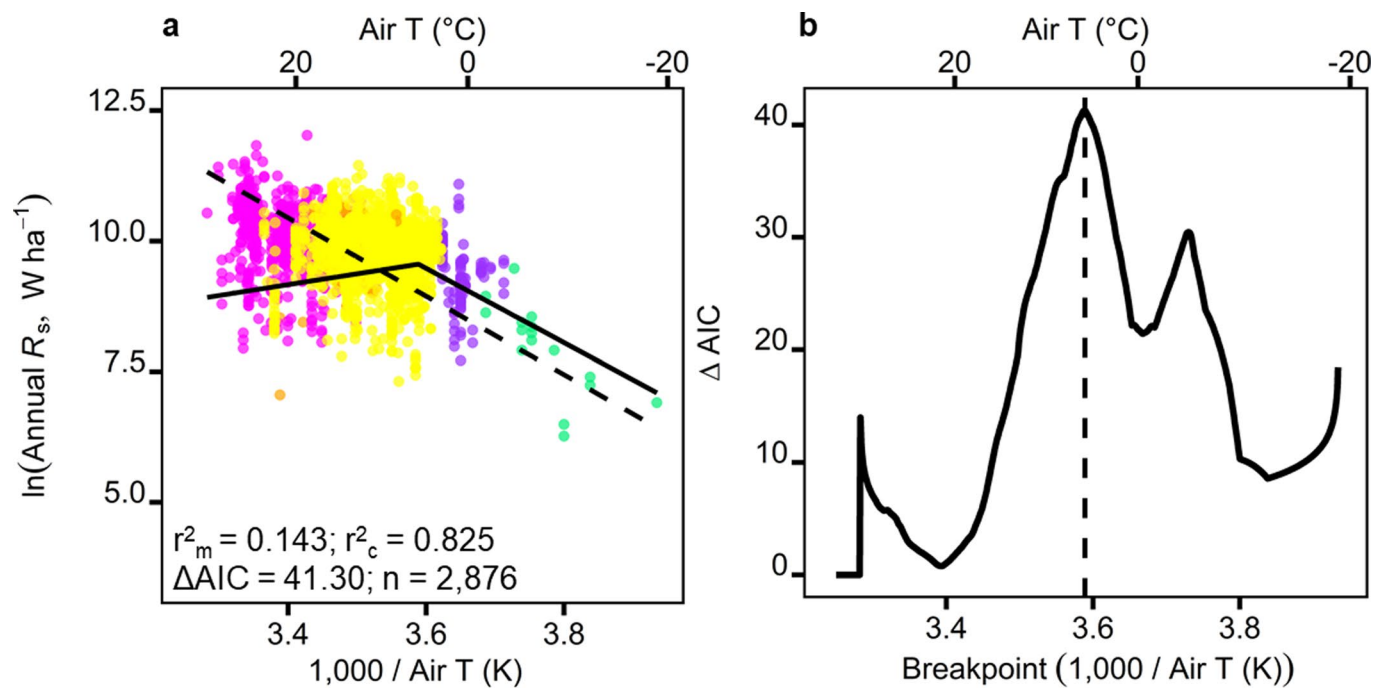


**Extended Data Fig. 3 | Threshold model for ecosystem respiration rates and air temperature when all low frequency temperature intervals were removed.** Threshold model for half-hourly ecosystem respiration rates and air temperature when all low frequency temperature intervals shown in Extended Data Fig. 2 (identified by asterisks) were removed from the dataset. Threshold model predictions (solid line, for the fixed effects of temperature only in a) identified a single temperature threshold of 14.6 °C, with little support for a second temperature breakpoint (b,  $\Delta\text{AIC} < 5$  and  $p > 0.05$ ). The dashed line in a indicate an activation energy of  $-7.50 \text{ K}$  as predicted by metabolic theory and  $\Delta\text{AICs}$  in b are between the linear and threshold model. Full details of the threshold mixed effects model are presented in Supplementary Table 3.



**Extended Data Fig. 4 | Correlation matrix between site variables and model goodness of fit.** Correlation matrix between FLUXNET site variables (latitude, maximum, minimum, mean and air temperature range (°C)) and the goodness of fit (adjusted *r*<sup>2</sup>) of the best performing model for predicting the temperature dependence of ecosystem respiration at the site level (threshold, *n* = 197; linear, *n* = 13; Supplementary Data 1).





**Extended Data Fig. 5 | Long-term temperature threshold for soil respiration.** Long-term temperature threshold for soil respiration ( $R_s$ ), showing a) mean annual  $R_s$  from the global soil respiration database (symbols, colours representing climate as in Fig. 2) and the threshold model prediction (solid line, for the fixed effects of temperature only); and b) identification of a single temperature breakpoint of  $5.5\ ^\circ C$ , with little support for a second temperature breakpoint ( $\Delta AIC < 5$  and  $p > 0.05$ ). Dashed lines indicate an activation energy of  $-7.50\ K$  as predicted by metabolic theory and  $\Delta AICs$  are between the linear and threshold model. Full details of the threshold mixed effects model are presented in Supplementary Table 6.

## Reporting Summary

Nature Research wishes to improve the reproducibility of the work that we publish. This form provides structure for consistency and transparency in reporting. For further information on Nature Research policies, see our [Editorial Policies](#) and the [Editorial Policy Checklist](#).

### Statistics

For all statistical analyses, confirm that the following items are present in the figure legend, table legend, main text, or Methods section.

n/a Confirmed

- ☐ ☒ The exact sample size ( $n$ ) for each experimental group/condition, given as a discrete number and unit of measurement
- ☒ ☐ A statement on whether measurements were taken from distinct samples or whether the same sample was measured repeatedly
- ☐ ☒ The statistical test(s) used AND whether they are one- or two-sided  
*Only common tests should be described solely by name; describe more complex techniques in the Methods section.*
- ☐ ☒ A description of all covariates tested
- ☒ ☐ A description of any assumptions or corrections, such as tests of normality and adjustment for multiple comparisons
- ☐ ☒ A full description of the statistical parameters including central tendency (e.g. means) or other basic estimates (e.g. regression coefficient) AND variation (e.g. standard deviation) or associated estimates of uncertainty (e.g. confidence intervals)
- ☐ ☒ For null hypothesis testing, the test statistic (e.g.  $F$ ,  $t$ ,  $r$ ) with confidence intervals, effect sizes, degrees of freedom and  $P$  value noted  
*Give  $P$  values as exact values whenever suitable.*
- ☒ ☐ For Bayesian analysis, information on the choice of priors and Markov chain Monte Carlo settings
- ☒ ☐ For hierarchical and complex designs, identification of the appropriate level for tests and full reporting of outcomes
- ☒ ☐ Estimates of effect sizes (e.g. Cohen's  $d$ , Pearson's  $r$ ), indicating how they were calculated

*Our web collection on [statistics for biologists](#) contains articles on many of the points above.*

### Software and code

Policy information about [availability of computer code](#)

Data collection No software was used

Data analysis R version 3.6.2 (12/12/2019)

For manuscripts utilizing custom algorithms or software that are central to the research but not yet described in published literature, software must be made available to editors and reviewers. We strongly encourage code deposition in a community repository (e.g. GitHub). See the Nature Research [guidelines for submitting code & software](#) for further information.

### Data

Policy information about [availability of data](#)

All manuscripts must include a [data availability statement](#). This statement should provide the following information, where applicable:

- Accession codes, unique identifiers, or web links for publicly available datasets
- A list of figures that have associated raw data
- A description of any restrictions on data availability

The data analysed during the current study is available on the FLUXNET website (<https://fluxnet.fluxdata.org/data/fluxnet2015-dataset/>) and is subject to data policy restrictions (<https://fluxnet.org/data/data-policy>). Summaries for each FLUXNET site are provided in Supplementary Data 1.

## Field-specific reporting

Please select the one below that is the best fit for your research. If you are not sure, read the appropriate sections before making your selection.

☐ Life sciences ☐ Behavioural & social sciences ☒ Ecological, evolutionary & environmental sciences

For a reference copy of the document with all sections, see [nature.com/documents/nr-reporting-summary-flat.pdf](https://www.nature.com/documents/nr-reporting-summary-flat.pdf)

## Ecological, evolutionary & environmental sciences study design

All studies must disclose on these points even when the disclosure is negative.

Study description	The study compiles night-time ecosystem respiration measurements from 210 FLUXNET sites. Factors included in this study for each site include air and soil temperature, site latitude and the site (for half-hourly measurements) or study year (for annual measurements), alongside ecosystem respiration rates.
Research sample	The study includes the compilation of existing FLUXNET datasets, acquired from <a href="https://fluxnet.org/data/">https://fluxnet.org/data/</a> and adhering to the data policy for Tier 2 Data.
Sampling strategy	Sample size for each site depended on the number of measurements available for both night-time ecosystem respiration rate and air or soil temperature.
Data collection	Data was collected from the existing FLUXNET datasets provided by <a href="https://fluxnet.org/data/">https://fluxnet.org/data/</a> . Measurements from each site were merged in to a single dataset for the factors included in the study.
Timing and spatial scale	The FLUXNET data were collected between 1991 and 2014, and span a latitudinal range from 78.92 °N to 37.43 °S.
Data exclusions	NA (-9999 values in FLUXNET) and negative values for night-time ecosystem respiration (RECO_NT_VUT_MEAN) were excluded from the merged dataset. NA values for air temperature (TA_F) or soil temperature (TS_F) were also excluded for the air and soil temperature analyses, respectively.
Reproducibility	Statistical analysis was fully reproduced when all data is analysed, as in this study.
Randomization	FLUXNET sites were allocated broad climate groups (tundra, boreal, temperate, mediterranean, and tropical), for which some generalizations were made. For instance, alpine sites were classified as boreal climates and subtropical sites were classified as either mediterranean or tropical depending on the site latitude and mean annual temperature.
Blinding	Blinding is not relevant to this study as we do not compare control and treatment groups.
Did the study involve field work?	<input type="checkbox"/> Yes <input checked="" type="checkbox"/> No

## Reporting for specific materials, systems and methods

We require information from authors about some types of materials, experimental systems and methods used in many studies. Here, indicate whether each material, system or method listed is relevant to your study. If you are not sure if a list item applies to your research, read the appropriate section before selecting a response.

### Materials & experimental systems

n/a	Involved in the study
<input checked="" type="checkbox"/>	<input type="checkbox"/> Antibodies
<input checked="" type="checkbox"/>	<input type="checkbox"/> Eukaryotic cell lines
<input checked="" type="checkbox"/>	<input type="checkbox"/> Palaeontology and archaeology
<input checked="" type="checkbox"/>	<input type="checkbox"/> Animals and other organisms
<input checked="" type="checkbox"/>	<input type="checkbox"/> Human research participants
<input checked="" type="checkbox"/>	<input type="checkbox"/> Clinical data
<input checked="" type="checkbox"/>	<input type="checkbox"/> Dual use research of concern

### Methods

n/a	Involved in the study
<input checked="" type="checkbox"/>	<input type="checkbox"/> ChIP-seq
<input checked="" type="checkbox"/>	<input type="checkbox"/> Flow cytometry
<input checked="" type="checkbox"/>	<input type="checkbox"/> MRI-based neuroimaging